Journal of proteome research

Article

pubs.acs.org/jpr

Characterization of the Interaction between Heterodimeric αvβ6 Integrin and Urokinase Plasminogen Activator Receptor (uPAR) Using Functional Proteomics

Seong Beom Ahn,[†,▽] Abidali Mohamedali,[‡,▽] Samyuktha Anand,[‡,▽] Harish R. Cheruku,[†] Debra Birch,[‡] Gopichandran Sowmya,[‡] David Cantor,[†] Shoba Ranganathan,[‡] David W. Inglis,[§] Ronald Frank,[∥] Michael Agrez,[⊥] Edouard C. Nice,[#] and Mark S. Baker*[,†]

[†]Australian School of Advanced Medicine, Faculty of Human Sciences, [‡]Department of Chemistry and Biomolecular Sciences, and [§]Department of Engineering, Faculty of Science, Macquarie University, Sydney, NSW 2109, Australia

[∥]Department of Chemical Biology, Helmholtz Centre for Infection Research, Inhoffen Strasse, 738124 Braunschweig, Germany

[⊥]Division of Surgery, John Hunter Hospital, Newcastle, NSW 2310, Australia

[#]Department of Biochemistry and Molecular Biology, Monash University, Melbourne, VIC 3800, Australia

ABSTRACT: Urokinase plasminogen activator receptor (uPAR) and the epithelial integrin αvβ6 are thought to individually play critical roles in cancer metastasis. These observations have been highlighted by the recent discovery (by proteomics) of an interaction between these two molecules, which are also both implicated in the epithelial−mesenchymal transition (EMT) that facilitates escape of cells from tissue barriers and is a common signature of cancer metastases. In this study, orthogonal in cellulo and in vitro functional proteomic approaches were used to better characterize the uPAR·αvβ6 interaction. Proximity ligation assays (PLA) confirmed the uPAR·αvβ6 interaction on OVCA429 (ovarian cancer line) and four different colon cancer cell lines including positive controls in cells with de novo β6 subunit expression. PLA studies were then validated using peptide arrays, which also identified potential physical sites of uPAR interaction with αvβ6, as well as verifying interactions with other known uPAR ligands (e.g., uPA, vitronectin) and individual integrin subunits (i.e., αv, β1, β3, and β6 alone). Our data suggest that interaction with uPAR requires expression of the complete αβ heterodimer (e.g., αvβ6), not individual subunits (i.e., αv, β1, β3, or β6). Finally, using in silico structural analyses in concert with these functional proteomics studies, we propose and demonstrate that the most likely unique sites of interaction between αvβ6 and uPAR are located in uPAR domains II and III.

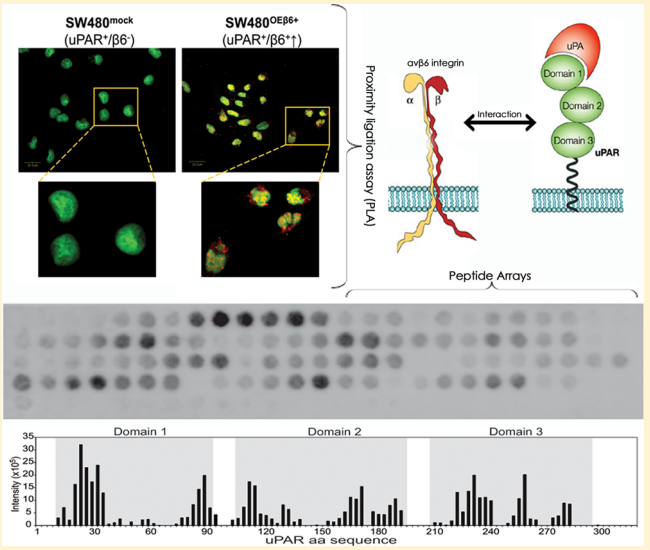

KEYWORDS: *functional proteomics, uPAR, αvβ6 integrin, proximity ligation assay, peptide array, ovarian cancer, colorectal cancer*

INTRODUCTION

A hallmark of epithelial cancer metastasis is the ability of cancer cells to migrate and infiltrate distant organs. Key stages during metastasis include detachment of the tumor cell from neighboring cells and the basement membrane, intravasation of cell(s) to the blood or lymphatic system, invasion of the migrated cell into a new environment, readhesion, and finally angiogenesis.[1] At the molecular level, the epithelial−mesenchymal transition (EMT) is thought to be a pivotal biological process that facilitates tissue remodeling and metastatic progression. Normal epithelial cells undergo numerous biochemical alterations during EMT, including loss of cell polarity, loss of cell−cell adhesion, suppression of E-cadherin, and an increase in cell migration and invasiveness.[2] EMT is facilitated by degradation of extracellular matrix (ECM) structures, allowing cancer cells to escape and potentially colonize secondary sites in the body.[2] Degradation of ECM is now thought to be one of the most complex and important mechanisms that drives EMT, but how this occurs is not yet fully understood. The matrix metalloproteinase (MMP) family and the serine protease plasminogen activation cascade are two major matrix degrading protease families implicated in epithelial cancer metastasis (e.g., breast, endometrial, hepato-

Received: August 15, 2014

   dx.doi.org/10.1021/pr500849x | J. Proteome Res. XXXX, XXX, XXX−XXX

cellular, colorectal, pancreatic, gastric, renal, brain, and lung).[3] Both the MMPs and the plasmin are found as inactive zymogens (pro-MMPs and plasminogen, respectively), which are spatially and temporally (spatiotemporally) activated in a series of steps.[4] Inactive plasminogen can be converted to active plasmin by urokinase plasminogen activator (uPA) on its major receptor the uPA-receptor (uPAR), where it is relatively "shielded" from inhibitors when located on the cell surface. Plasmin degrades many ECM components including fibrin, fibronectin, laminin, and the protein core of proteoglycans,[4] while also activating MMP-1, MMP-3, and MMP-9 among many proteases that consequently degrade additional ECM components.[3] To understand the regulation and consequences of ECM degradation in the tumor microenvironment, it was essential to determine cell surface interacting proteins. Using immunoprecipitation and mass spectrometry, we recently elucidated a cell surface uPAR interactome using an ovarian cancer cell line (OVCA429) with the novel discovery of the interaction of uPAR and integrin $\alpha v\beta 6$,[5] subsequently shown as uPAR·$\alpha v\beta 6$. This was further validated by Western blot analysis. Interestingly, both of these cell surface proteins have been implicated in many aspects of the biology of epithelial cancer and its progression.[5]

From more than 8000 membrane proteins predicted from the human protein-coding genes,[6] uPAR has been suggested to be one of a few multifunctional multi-interacting cell surface receptors that is known to be involved in, among other things, ECM degradation, growth factor activation, and downstream cellular signaling.[7] A glycosylphosphotidylinositol (GPI) linker anchors the three domains (DI, DII, and DIII) of the mature uPAR protein to the extracellular surface of the plasma membrane. These three domains form a thick-fingered glove-like structure that provides a central pocket for the binding of the cognate ligand protease, uPA.[8] Equally this shape reveals a large contralateral external surface potentially facilitating interactions with other proteins.[8] While initial studies focused exclusively on regulation of plasmin activation by uPAR, 42 proteins (9 extracellular proteins and 33 lateral interacting partners) have now been proposed to interact with uPAR.[9] This exhaustive list suggests that uPAR may have evolved multiple different ligand specificities involved in the regulation of many biologies, like proteolysis, cell migration, proliferation, cell signaling, as well as other yet to be explored cell behaviors. Indeed, in the past decade, extensive evidence has suggested that uPAR is implicated in cell adhesion, proliferation, migration, tissue remodeling, and regulation of signaling pathways (e.g., MAP kinase, Ras pathways),[7] which are important features not only of ubiquitous developmental pathways, but more importantly for cancer metastasis. High expression of the uPAR antigen has been observed in many cancers (including breast, ovarian, colon, and lung[10,11]). In colorectal cancer (CRC), a high level of uPAR has been suggested as a prognostic factor for poor survival.[11] Additionally, up-regulation of uPA in metastasis and its subsequent roles in the degradation of the ECM have further suggested uPAR and its interacting partners are central to processes that lead to metastasis, including EMT.[12]

As uPAR possesses no intrinsic intracellular domain, it is commonly thought that downstream cellular signaling pathways influenced by uPAR must be mediated through lateral interactions with transmembrane proteins (e.g., integrins). Indeed, 11 integrins (out of a total of 24) have been suggested to directly interact with uPAR,[9] and many of these studies have implicated these interactions in some role in cancer metastasis.[13] A major function of integrins that relates them directly to cell adhesion in cancer metastasis is in cellular traction, where the β subunit embeds itself across the cell membrane and mechanically links integrins to the cytoskeleton and ECM.[13] Integrins also regulate molecular processes related to cell morphology, proliferation, survival, migration, and invasion, mostly by engaging in crucial intracellular signaling.[13]

This study focuses specifically on the $\alpha v\beta 6$ integrin, a transmembrane heterodimer receptor expressed exclusively on the surface of epithelial cells. The $\alpha v\beta 6$ integrin is involved in a bidirectional manner in the signal cascade system, sending signals from the cells to the ECM and vice versa via a series of protein binding partners, which include fibronectin, cytotactin, tenascin, vitronectin (Vn), and TGFβ1.[14] High expression of $\alpha v\beta 6$ has been demonstrated in various cancers including CRC, liver, ovarian, gastric, thyroid, cervical squamous, and endometrial cancer, where its expression is often correlated with poor patient survival.[15,16] Several studies have implicated $\alpha v\beta 6$ in cell proliferation, migration, and invasion,[16,17] with some reports suggesting the involvement of $\alpha v\beta 6$ through activation and up-regulation of various MMP-driven proteolytic pathways.[16] Furthermore, it has been conclusively demonstrated that $\alpha v\beta 6$ activates nascent latent transforming growth factor, TGF-β1,[18] which can also up-regulate MMP pathways,[19] leading to similar outcomes.

Our central hypothesis here is that, when coexpressed, uPAR and $\alpha v\beta 6$ function cooperatively as a single membrane proteomic machine (as uPAR·$\alpha v\beta 6$). In this study, we confirm the originally observed uPAR·$\alpha v\beta 6$ interaction by functional proteomics using two orthogonal techniques, proximity ligation assays (PLA) and peptide arrays. In detail, PLA is an in cellulo technique that allows direct detection of protein−protein interactions due to the close proximity of the binding partners, and the in vitro peptide array method was used to locate potential specific interacting sites in uPAR·$\alpha v\beta 6$ using an offset 15-mer sequential array of uPAR peptides across the whole protein sequence to find binding sites using HRP-labeled $\alpha v\beta 6$ or other ligands (i.e., uPA, Vn, and integrin subunits). Furthermore, using an in silico structural analysis tool (ICM bioinformatics software), we were able to map putative sites of uPAR and $\alpha v\beta 6$ interaction. This study not only validates the uPAR·$\alpha v\beta 6$ interactions observed by proteomics in CRC and ovarian cancer cells, but also opens significant new avenues for functional targeting of similar interactions that may play key roles in epithelial cancer metastasis and provide unique therapeutic options.

MATERIALS AND METHODS

Antibodies and Recombinant Proteins

Monoclonal antibodies (mAb) against human uPAR (clone R4, IgG1) were purchased from DAKO (Glostrup, Denmark). The mAb against the $\beta 6$ subunit of the human $\alpha v\beta 6$ integrin (clone 6.4B4, IgG1) was obtained from Biogen Idec (Cambridge, MA).[20] Isotype control, IgG1, was purchased from R&D Systems (Minneapolis, MN). The full length recombinant proteins that were used for the peptide array were uPA and integrin $\alpha v\beta 6$ (R&D Systems); vitronectin (Merck Millipore, MA); and integrin αv, $\beta 6$, $\beta 1$, and $\beta 3$ (Abnova, Taipei City, Taiwan).

dx.doi.org/10.1021/pr500849x | J. Proteome Res. XXXX, XXX, XXX−XXX

Cell Culture

The ovarian and colon cancer cell lines expressing uPAR and varying levels of $\beta6$ used for the experiments were: ovarian, OVCA429[21] (uPAR$^+$, $\beta6^+$); colorectal, HT29^{mock} (uPAR$^+$, $\beta6^+$), HT29$^{\beta6AS}$ (uPAR$^+$, $\beta6^+\downarrow$), SW480$^{\beta6OE}$ (uPAR$^+$, $\beta6^+\uparrow$), and SW480^{mock} (uPAR$^+$, $\beta6^-$).[22,23] The OVCA429 cells were cultured in DMEM (Invitrogen) media supplemented with 10% FBS, 100 μg/mL penicillin, 100 μg/mL streptomycin, 10 mM HEPES, and 6 mM L-glutamine. The HT29^{mock} and HT29$^{\beta6AS}$ cells were cultured in RPMI media (Invitrogen, San Diego, CA) supplemented with 10% FBS and 2.5 μg/mL puromycin. The SW480$^{\beta6OE}$ and SW480^{mock} cells were cultured in DMEM supplemented with 4.5 g/L glucose, 10% FBS, and 500 μg/mL Geneticin G418 (Invitrogen). The cells were seeded at 2×10^5 cells/mL and were grown until ~50% confluence prior to immunofluorescence and PLA experiments. All cells were grown at 37 °C in 5% CO_2 (v/v) in biological triplicates.

Immunofluorescence (IF)

The presence and/or absence of uPAR and $\beta6$ in all five cell lines were confirmed using IF. When cell cultures reached ~50% confluence, the cells were fixed using 2% paraformaldehyde for 10 min, washed with 0.1 M glycine in PBS, and incubated with blocking solution (9% goat serum, 1% BSA in PBS) for 1 h at room temperature. The cells were then incubated with anti-uPAR R4 (5 μg/mL) and anti-$\alpha v\beta6$ 6.4B4 (5 μg/mL) antibodies for 1 h at 37 °C followed by incubation with Alexa Fluor 488 goat Anti-Mouse IgG (H+L) (Invitrogen) as secondary antibody (4 μg/mL), for 1 h at 37 °C. Cell nuclei were counter stained with the blue fluorescent DAPI (Invitrogen) nucleic acid stain (300 nM) for 10 min and mounted on glass slides in Gelmount (ProScitech, Australia). The cells were analyzed using a UPLSAPO 40× objective (NA. 0.95) on a fluorescence microscope (BX63, Olympus, Tokyo). All image capture was conducted using a XM10, monochrome cooled CCD camera and CELLSENS dimensions software (Olympus, Tokyo).

Proximity Ligation Assay (PLA)

The assay was performed according to manufacturer's instructions (Olink Bioscience, Uppsala, Sweden). Briefly, the PLUS oligonucleotide probe was conjugated to anti-uPAR R4 and its isotype control (IgG1), while the MINUS oligonucleotide probe was conjugated to anti-$\alpha v\beta6$ 6.4B4 and its corresponding isotype control (IgG1). Cells were fixed using 2% paraformaldehyde in PBS and blocked using blocking solution (9% goat serum, 1% BSA in PBS). Oligonucleotide probe conjugated antibodies were introduced to the cells and incubated for 1 h, followed by incubation with the ligation solution for 30 min, followed by amplification solution (contains Cy5 fluorophore) for 100 min. Cells were counter stained with SYBR Green1 stain and mounted. The PLUS and MINUS oligonucleotide conjugated IgG1 mAbs were used as negative controls.

PLA Imaging

The cells were imaged using an Olympus Fluoview 300 confocal laser scanning system equipped with an inverted microscope (IX70, Olympus Tokyo). A 40× UPLAN APO objective (NA 0.95) was used for analysis of all slides. SYBR Green1 stain was excited using a 488 nm argon laser and the emission signal detected using 510 and 530 nm interference filters. The Cy5 dye was excited using the 633 nm HeNe laser, and the emission signal was detected using a long pass 610 barrier filter. Three sets of images, in the X, Y, and Z dimensions (10 optical slices with a spacing of 0.5 μm), were captured for each replicate and image analysis performed on the extended XYZ images, using Duolink Image Tool software (Olink Bioscience). The number of protein interaction signals (seen as red spots) per cell was calculated for each image. Aggregated cells were counted manually to avoid miscalculation. A student t test was performed to establish the statistical significance of uPAR·$\alpha v\beta6$ for each cell line.

uPAR Peptide Array

A cellulose-bound array of 108 spots of 15-mer peptides covering the complete uPAR sequence of 331 amino acids with a 3 amino acid shift was synthesized using SPOT synthesis.[24,25] The uPAR peptide arrays were blocked with 5% skim milk followed by incubation with HRP conjugated recombinant proteins (HRP-RPs) for 4 h. HRP-RPs were prepared by a Lightning-Link HRP conjugation kit (Innova Biosciences) as per the manufacturer's instructions. Unbound HRP-RPs was washed off, and bound HRP-RPs was detected using Super-Signal West Femto Chemiluminescent Substrate (Thermo Scientific). Images were captured using a Fujifilm CS3000 imager in chemiluminescence mode with the intensity adjusted such that the darkest spots were slightly below saturation. The images were then analyzed using MultiGuage software (FujiFilm). A quantitative intensity value for each spot was calculated using the following formula:

$$\text{intensity} = (\text{AU} - \text{BG})/t$$

where "AU" is the measured intensity of each spot, "BG" is the background, and "t" is the time of exposure of the imaging. The uPAR peptide array with $\alpha v\beta6$ was performed in triplicate to confirm reproducibility.

Bioinformatics Analysis of uPAR Interaction

The known crystal structures (PDB ID: 3BT1) of uPAR, uPA, and Vn complex[26] were analyzed using the ICM bioinformatics software (Internal Coordinate Mechanics).[27] First, the uPAR regions that bound to $\alpha v\beta6$ on the peptide array were graphically visualized using ICM. These regions were then subjected to manual analysis to determine residues with favorable side-chain orientations. The residues with favorable side-chain orientations were then reanalyzed to determine $\alpha v\beta6$ residues potentially accessible to the outer surface of uPAR based on hydrophobicity.

RESULTS AND DISCUSSION

Previous proteomics studies using immunoprecipitation, mass spectrometry, and Western blot analysis, using the ovarian cancer cell line OVCA429,[5] demonstrated that uPAR potentially interacts with other membrane associated proteins, including the $\alpha v\beta6$ integrin heterodimer. Many of the proteins identified in that study had been previously implicated in either the biology of cancer metastasis, the regulation of plasminogen activation, or as prognostic indicators of poor cancer patient survival (e.g., α-enolase, $\alpha v\beta6$, uPAR). Specifically, uPAR and $\alpha v\beta6$ have been independently implicated in both cancer biology (e.g., proliferation, TGFβ activation, cell adhesion, migration, proteolysis, and invasion) and poor epithelial cancer patient prognosis (colorectal, breast, prostate, lung, and ovarian cancer).[7] Coexpression of uPAR and $\alpha v\beta6$ in the OVCA429 and other cell lines is now well established.[5] Studies using flow cytometry have also independently confirmed the expression of

dx.doi.org/10.1021/pr500849x | J. Proteome Res. XXXX, XXX, XXX−XXX

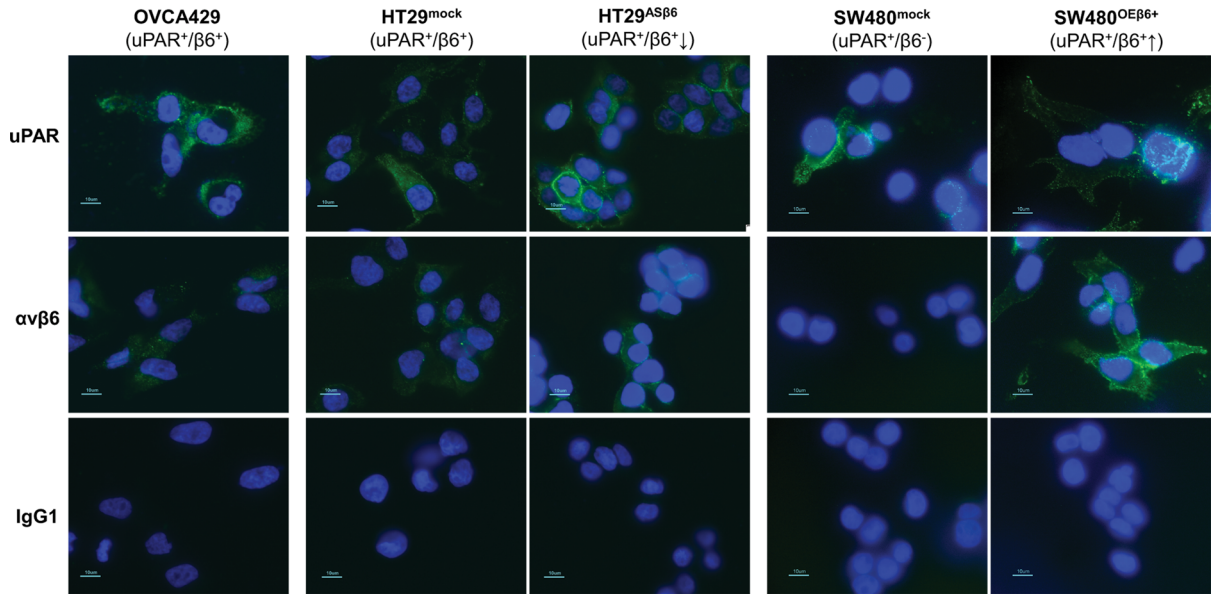

Figure 1. A representation of the cell surface expression of uPAR and $\alpha v\beta 6$ for five different cell lines as SW480 $\beta 6$OE, SW480 mock, OVCA-429, HT-29 mock, and HT-29 $\beta 6$AS each expressing varying levels of $\beta 6$. The third row represents the antibody control (IgG1). Nuclei were stained with DAPI, while proteins were detected with a secondary antibody conjugated to Alexa 488.

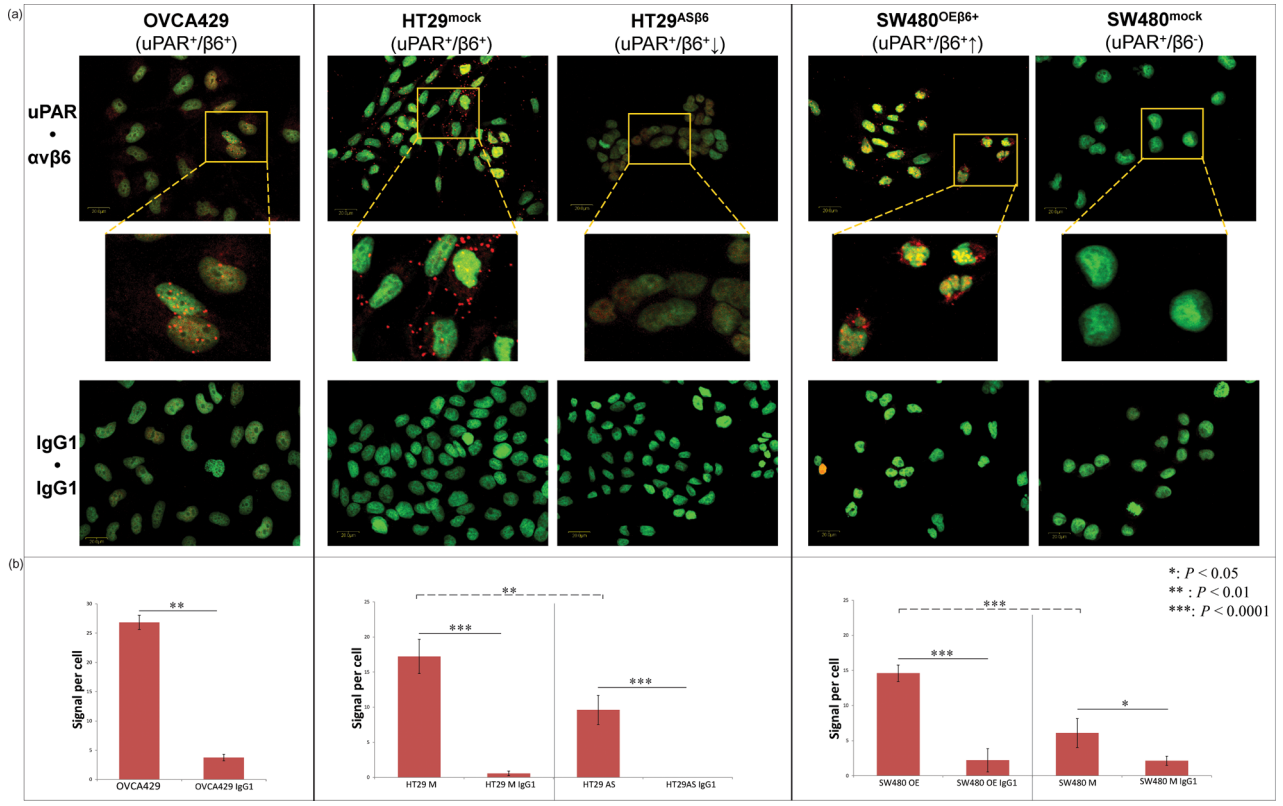

Figure 2. Proximity ligation assay images of the cells shown in (A) where the red spots represent the interaction between uPAR·$\alpha v\beta 6$. A signal for the interaction of the uPAR·$\alpha v\beta 6$ corresponding to the level of $\beta 6$ in the cell seems to be observed as compared to the IgG1 isotype control. (B) This observation was quantified by measuring the number of spots per cell. The results showed a significant decrease in interaction when the level of $\beta 6$ was reduced by 35% (in HT-29 $\beta 6$AS cells) ($p < 0.05$). Similarly, a significant increase in interactions was observed when $\beta 6$ was up-regulated in SW480 $\beta 6$OE cells.

both of these antigens on the cell surface.[23,28−30] However, correlations of tumor tissue coexpression and relationships with cancer stage, differentiation status, and patient clinical outcomes (including survival) remain to be explored. The confirmation of a direct uPAR·$\alpha v\beta 6$ interaction would suggest a novel paradigm that potentially explains how and why these membrane proteins share critical aspects of tumor biology and would assist in the development of novel therapeutics to prevent cancer metastasis.[29]

dx.doi.org/10.1021/pr500849x | J. Proteome Res. XXXX, XXX, XXX−XXX

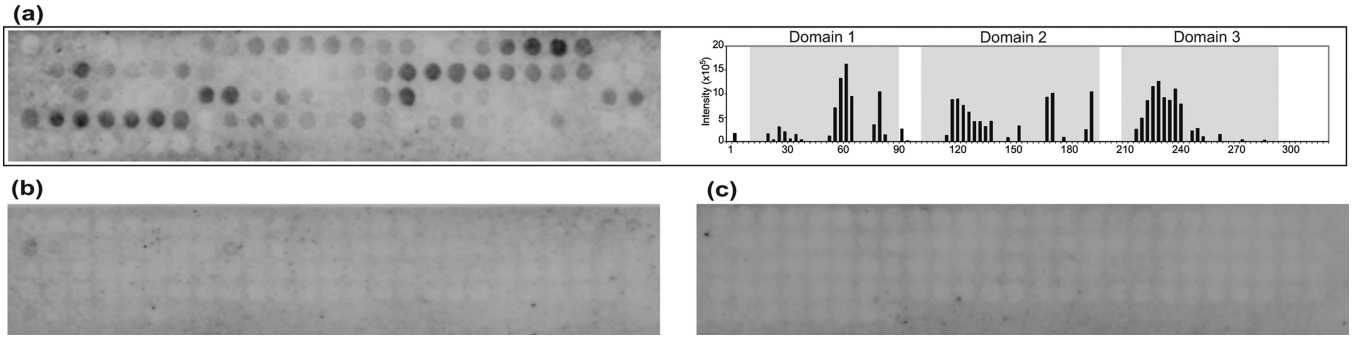

Figure 3. (a) uPAR peptide array incubated with $\alpha v\beta 6$ and corresponding intensity plot indicating locations of binding on the three domains of uPAR with the more intense spot (semiquantitatively indicated on the bar chart) indicating a stronger affinity for the heterodimer to the corresponding uPAR peptide. The same peptide array incubated with αv (b) and $\beta 6$ (c) integrins separately, neither of which showed any binding to the array.

The aim of the present study was to functionally validate our previous proteomic studies[5] on IP pull downs of the specific interacting sites of uPAR·$\alpha v\beta 6$ by using two diverse orthogonal biochemical techniques: PLA for in cellulo studies and peptide arrays for in vitro analysis of the specific interacting sites. To validate the uPAR·$\alpha v\beta 6$ interaction, ovarian (OVCA429) and four colon cancer cell lines were employed (HT29^{mock}, HT29$^{\beta 6AS}$, SW480$^{\beta 6OE}$, and SW480^{mock}). The dysregulation of uPAR and $\beta 6$ in these cell lines has been previously demonstrated by various techniques not limited to but including flow cytometry, Western blot, and PET analysis.[29,31−33]

Immunofluorescence and PLA Confirm the Presence of uPAR·$\alpha v\beta 6$ Interactions

In this study, immunofluorescence (IF) was used to demonstrate the presence of uPAR and $\alpha v\beta 6$ on the cell surface using anti-uPAR R4 and anti-$\alpha v\beta 6$ 6.4B4 mAbs. Consistent with previous studies, these results demonstrated that uPAR was expressed on the cell surface of all cell lines, while $\alpha v\beta 6$ was expressed on SW480$^{\beta 6OE}$, HT29^{mock}, HT29$^{\beta 6AS}$, and OVCA429, but was not on SW480^{mock} (Figure 1). No binding (no fluorescence) was observed with the negative isotype control IgG1 antibody (Figure 1) as control.

Proximity ligation is an emerging technology that has been used to visualize and simultaneously quantify P·P interactions occurring in situ.[34] Proteins in close proximity (30−40 nm) are fluorescently detected using rolling circle amplification of ligatable DNA primers attached to secondary antibodies that bind a pair of epitope-specific monoclonal antibodies.[34,35] In our study, primary antibodies were directed against uPAR and $\alpha v\beta 6$. Expression of integrin $\beta 6$ is restricted to epithelial cells, and it is only known to dimerize with the αv subunit.[36] Therefore, to identify whether interaction with uPAR could be demonstrated quantitatively, we examined other cell lines in which relative expression levels of the $\beta 6$ integrin were modulated. The cell lines used expressed uPAR with varying levels of integrin $\beta 6$ expression. For example, cells that did not express $\beta 6$ (i.e., SW480^{mock}) were compared to those in which integrin $\beta 6$ had been engineered to be overexpressed (SW480$^{\beta 6OE}$). In addition, cells that endogenously expressed $\beta 6$ (HT29^{mock}) were compared to subclones of the same cell line in which $\beta 6$ expression had been deliberately and stably reduced by ∼80% (i.e., HT29$^{\beta 6AS}$)[29] (Figure 2).

To allow statistical analyses, the assay was performed in biological triplicate for all cell lines, and three images were acquired for each replicate. A significant number of positive spots were observed localized to the cell surface as anticipated (Figure 2). The OVCA429, SW480$^{\beta 6OE}$, and HT29^{mock} cell lines showed strong signals for the uPAR·$\alpha v\beta 6$ interaction, whereas the HT29$^{\beta 6AS}$ cell line showed much weaker signals ($p < 0.05$) (Figure 2a), which is in agreement with the reduced $\beta 6$ expression previously reported.[29] The SW480^{mock} cell line, where $\beta 6$ is completely absent, showed no apparent uPAR·$\alpha v\beta 6$ PLA signal (Figure 2a). An analysis of the average signal obtained per cell as compared to the corresponding isotype controls demonstrated that the signals obtained from uPAR·$\alpha v\beta 6$ were significantly greater ($p < 0.05$) than the control (Figure 2b).

The results for the OVCA429 cell line were similar to those we had obtained previously.[5] For the colon cancer cell lines, PLA data showed a significant decrease in interaction when the level of $\alpha v\beta 6$ was reduced; concordantly, a significant increase in interaction was observed when $\alpha v\beta 6$ was up-regulated.

In all cases, our PLA results were in good agreement with previous expression data,[29] showing that quantitative uPAR·-$\alpha v\beta 6$ PLA signal could be altered simply by decreasing or increasing the expression level of $\beta 6$ present on the cell surface. All isotype controls were negative. However, while collectively these data show close proximity of uPAR and $\beta 6$ indicative of an interaction, the possibility that other "bridging" proteins may be involved in direct interactions with either partner in uPAR·$\alpha v\beta 6$ could not be conclusively excluded. To eliminate this possibility, direct uPAR·$\alpha v\beta 6$ was probed using an orthogonal technique, peptide arrays.

Peptide Arrays Map Potential Sites of uPAR·$\alpha v\beta 6$ Interaction

Peptide arrays are cost-efficient, accurate, and reliable one-dimensional reconstructions that allow mapping of potential peptidyl binding sites of labeled full length interacting proteins.[37] They have been widely used to analyze large arrays of synthetic peptides on cellulose membranes, facilitating the rapid screening of diverse biomolecule probes.[38] SPOT synthesis[24] was used in this study to generate an array composed of 108 sequential overlapping (3 residues) 15-mer peptides (along the linear uPAR expressed protein sequence) arranged successively on a cellulose membrane. This was used to map the potential binding sites of uPAR and the heterodimeric $\alpha v\beta 6$ integrin, as well as the individual integrin subunits (αv and $\beta 6$). While this method involves a reduction of the three-dimensional uPAR structure into single linear overlapping 15-mer peptides, the method has been used

dx.doi.org/10.1021/pr500849x | J. Proteome Res. XXXX, XXX, XXX−XXX

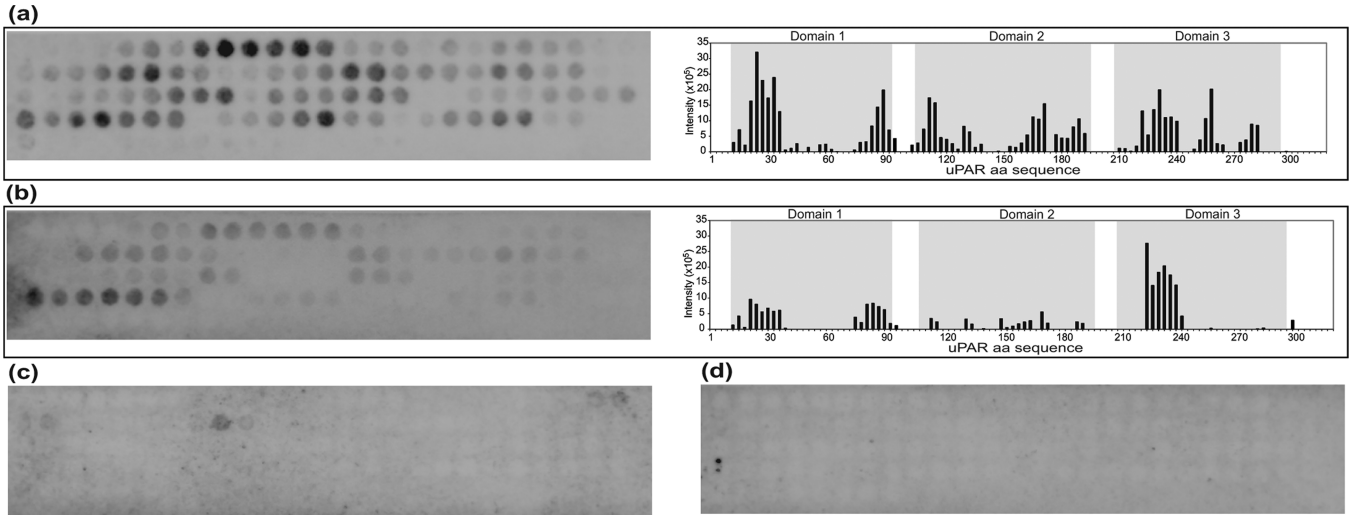

Figure 4. (a) uPAR peptide array incubated with uPA and corresponding intensity plot indicating locations of binding on the three domains of uPAR with the more intense spot (semiquantitatively indicated on the bar chart) indicating a stronger affinity for the heterodimer to the corresponding uPAR peptide. The same peptide array incubated with vitronectin, another known binding partner of uPAR, and its corresponding intensity plot (b) and the β1 (c) and β3 (d) integrins separately, neither of which again, as monomers, showed any binding to the array.

Table 1. Potential uPAR and Integrin $\alpha v\beta 6$ Interaction Sites[a]

uPAR domain	region identified from peptide array	possible surface residues identified	overlapping residues binding to Vn (uPA)
I	**61** ELVEKSCTHSEKTNRTLS **78**	E61, V63, K65, S70, E71, N74, T76, S78	S78 (T76)
	82 GLKITSLTEVVCGLD **96**	I85, S87, T89, V91, L95	I85, S87 (T89)
II	**121** GSSDMSCERGRHQSLQCRSPE **141**	M125, R129, R131, H132, S134, Q136, R138	Q136, R138
	172LPGCPGSNGFHNNDTFHF **189**	S178, N184, D185, F187, F189	none
	193 CNTTKCNEGPILELE **207**	N194, T195, K197, E200, P202, E207, N208	none
III	**229** SEETFLIDCRGPMNQCLVATGTHEPKN **255**	S229, E230, L234, D236, D238, N242, Q243, V246, T248, T250, T254	none

[a]Regions binding to integrin $\alpha v\beta 6$ on the peptide array and possible surface residues were identified by manual analysis of the uPAR crystal structure. The last column lists known overlapping binding residues to Vn and uPA (in parentheses). Amino acid residue numbers correspond to full uPAR sequence from UniProt KB (ID: Q03405).

successfully to identify linear specific binding sequences involved in many P·P interactions.[24]

In this study, a GUI (graphical user interface) was developed to semiquantitatively determine the binding affinity of the labeled species (e.g., HRP-labeled $\alpha v\beta 6$) to the uPAR peptide array based on the intensity of positive spots identified (Figure 3a). Overall, our data showed that integrin $\alpha v\beta 6$ binds to peptides emanating from all three uPAR domains (DI, DII, and DIII); in particular, positive binding of labeled-$\alpha v\beta 6$ was located within the following uPAR amino acid sequences: uPAR DI at E61-R75 and G82-D96, uPAR DII at G121-E141, L172-F189, and C193-E207, and uPAR DIII at S229-N255.

In control experiments using identical protein concentrations, the individual integrin protein subunits αv (Figure 3b) or $\beta 6$ (Figure 3c) did not bind to any region of the uPAR peptide array, in contrast to the $\alpha v\beta 6$ dimer.

The peptide array was also used to identify the binding sites of other potential uPAR partners, uPAR's cognate protease ligand uPA and the well-established binding partner Vn. The integrin subunits β1 and β3 were also examined to determine if they were able to bind as individual integrin subunits in contrast to the data observed for $\beta 6$ (Figure 3C).

These data showed that uPA could bind through domain I, C16-V51, I85-T108; domain II, S112-H150, C169-P210; and domain III, M226-Y258 and I283-V300, (Figure 4a), while Vn was found to bind to domain I, G22-V51, G82-R105; domain II, L116-H150, L172-E207; and domain III, G226-N255 (Figure 4b). As observed for individual subunits αv and $\beta 6$, neither β1 nor β3 (Figure 4c and d) showed any detectable binding to the uPAR peptide array.

Structural Mapping of Interacting Sites Reveals Pockets of uPAR·$\alpha v\beta 6$ Interactions

Six potential binding sites were located on the uPAR sequence from the collective peptide array data. These sites were found to be spread across all three domains of uPAR and covered almost 35% of the uPAR sequence. Interestingly, a number of the sequences found to bind to $\alpha v\beta 6$ integrin have previously been implicated in interactions with either Vn and/or uPA (Table 1).[7] To narrow potential docking/binding sites for integrin $\alpha v\beta 6$, an in silico structural analysis of where these six sites were located on the uPAR crystal structure was undertaken and mapped using ICM software (Figure 5a). This was followed by a manual identification of uPAR regions with residues containing favorable side-chain orientations and then investigated for potential residues that could be accessed on the outer surfaces of uPAR (Table 1).

Initial uPAR residue side-chain orientation analysis revealed that approximately 39% of the $\alpha v\beta 6$ interacting uPAR residues identified on peptide arrays possessed side chains found in favorable orientations (i.e., surface accessible). However,

dx.doi.org/10.1021/pr500849x | J. Proteome Res. XXXX, XXX, XXX−XXX

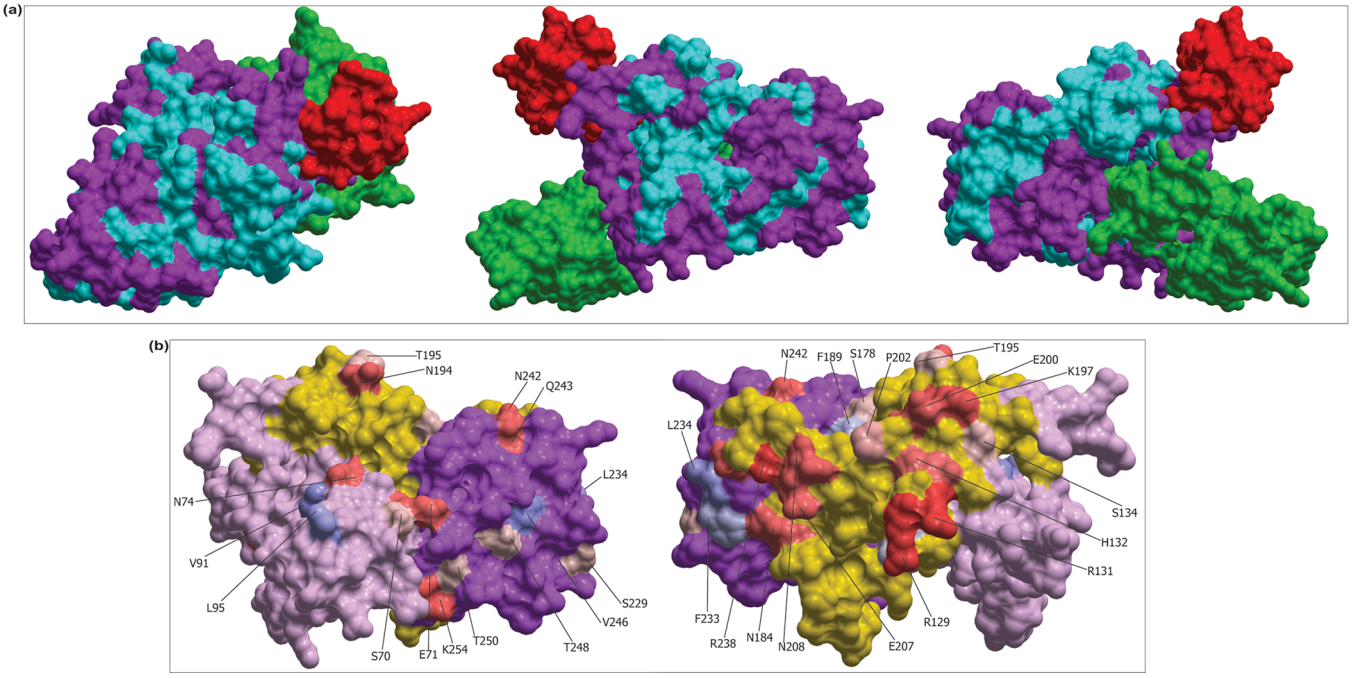

Figure 5. (a) The space-filling crystal structure of uPAR (magenta) with red indicating vitronectin, green indicating uPA, and cyan showing regions of uPAR binding to $\alpha v\beta 6$ from uPAR peptide array in three different views. (b) Crystal structure of uPAR only indicating its three domains (light pink, domain I; yellow, domain II; magenta, domain III) overlaid with predicted hydrophobicity labeled in red (residues with H-bond acceptor potential) and blue (residues with H-bond donor potential). The intensity of red and blue shows how strong or weak the H-bond formation potential is, and the numbers correspond to the amino acid sequence of uPAR without the signal peptide. A total of 14 potential residues as sites of binding can be observed on domain II, while 11 can be observed on domain III.

further manual analysis revealed that many of these residues were inaccessible. Only the favorable residues were then subjected to physicochemical (hydrophobicity) analysis (Figure 5). Figure 5b illustrates the hydrophobic nature of the residues identified. It was noted that most of the identified residues had hydrogen (H-) bond acceptor potential (red residues) with some residues having the potential to be H-bond donors (blue residues), while very few residues showed any potential to form H-bonds. Those with acceptor or donor H-bond potentials should prove better binding sites than those with low or no H-bond acceptor potential.

It was clear from this analysis that some residues identified in regions of uPAR domain I (E61 to R75 and G82 to D96) that had been previously suggested to be required for interaction with Vn and/or the receptor's cognate protease ligand uPA[26,39] were buried inside the outer surfaces of uPAR. Residues Q136 and R128, and L172, P173, and H188 in uPAR domain II, which have been previously demonstrated to be required for interaction with Vn and uPA, respectively, were found to be surface accessible.[26,39]

This study revealed that most of the domain II and III residues identified from the arrays could potentially be sites of $\alpha v\beta 6$ integrin interaction. Interestingly, a previous study addressing interactions between integrin $\alpha 5\beta 1$ and uPAR suggested that integrin $\alpha 5\beta 1$ directly interacts with uPAR domain III across the sequence G262-Q270 and the interaction was lost when a single amino acid alanine substitution (S267A) was introduced.[40] Our data suggest that although domains II and III maybe accessible for integrin binding, domain III appears to be a more favorable site, should other ligands be available.

While binding of uPA to its cognate receptor uPAR is a high affinity interaction ($K_d = 4 \times 10^{-10}$ M),[41] significant external regions of uPAR remain available for binding to other potential interacting partners (e.g., Vn and various integrins like $\alpha 3\beta 1$, $\alpha_M\beta 2$, $\alpha v\beta 1$, $\alpha 5\beta 1$, $\alpha v\beta 3$[42]). The uPA and Vn sites indicated from the peptide array showed ~70% overlap with binding sites already published,[26,39] including data obtained from alanine scanning mutagenesis experiments.[9] A detailed structural docking study has been performed to recapitulate and confirm these findings on the interaction of uPAR and $\alpha v\beta 6$.[43]

IMPLICATIONS AND FUTURE DIRECTIONS

The most likely binding sites for $\alpha v\beta 6$ to uPAR, based on the crystal structure of uPAR (bound to uPA and Vn) coupled with information arising from our peptide array data and a manual analysis of potential binding sites by side-chain orientation and hydrophobicity, appeared to be neighboring adjacent integrin binding sites that were previously identified.[40] An additional advantage of the use of peptide arrays in this study over screening by site directed protein−protein interaction libraries or molecular modeling is that not only are potential binding sites identified, but lead peptide antagonists also determined. These can subsequently be used as tools to address the specific interaction under study.[44] Structural analysis coupled with the previous study on interaction of uPAR with $\alpha 5\beta 1$[40] suggests that uPAR domain III may be a favorable binding site for "all" uPAR-binding integrins. Experiments using blocking peptides against the domain III region of uPAR to determine the precise binding site of uPAR and integrin $\alpha v\beta 6$ are currently ongoing.

For cell motility, invasion, proliferation, and adhesion, it is essential for uPAR to interact with transmembrane proteins for transmission of specific signals across cell membranes to activate appropriate intracellular second messenger systems. Thus, interaction of uPAR with $\alpha v\beta 6$ and other integrins not

dx.doi.org/10.1021/pr500849x | J. Proteome Res. XXXX, XXX, XXX−XXX

only couples the proteolytic activation (by binding with uPA) with cell signaling but also localizes the proteolysis to the cell surface.[7] Interactions between uPAR and $\alpha v\beta 6$ could potentially have profound implications on the promotion of cancer cell metastasis by activating a series of specific signaling pathways. For example, uPAR is involved in the Ras-ERK pathway, which is known to directly induce EMT in cells.[7,45] The association of uPAR with integrins like $\alpha 3\beta 1$, $\alpha v\beta 1$, $\alpha 5\beta 1$, $\alpha v\beta 3$ has been studied to varying degrees. It has been shown that uPAR interaction with $\beta 1$ activates both FAK and ERK/MAPK pathways,[40] while interaction with $\beta 3$ activates the Rac pathway.[46] Similarly, studies have shown that disruption of a uPAR and $\alpha v\beta 3$ integrin interaction selectively inhibits Vn-induced cell migration,[9,47] implying that $\alpha v\beta 6$ might also modulate cell migration in some comparable manner.

High expression of $\alpha v\beta 6$ is associated with poor prognosis in many cancer types, including colon cancer.[48] Several studies have implicated $\beta 6$ in cell proliferation, migration, and invasion,[49−51] although the mechanisms by which these processes occur remain unclear. Some reports have suggested involvement of $\alpha v\beta 6$ in MMP pathways as a means by which ECM degradation is facilitated.[16,52] For example, Fyn kinase, which associates with $\alpha v\beta 6$, recruits FAK, thereby activating the Rac/ERK/MAPK pathways, which in turn activate MMP3.[50] There is also evidence showing that $\alpha v\beta 6$ activates transforming growth factor TGF$\beta 1$ by a mechanism involving torsional stress (not proteolysis), which leads to up-regulation of MMP pathways.[53] In addition, a direct interaction between $\alpha v\beta 6$-P-ERK2 has been conclusively established[29] and shown to mediate MMP-9 secretion in colon cancer cells.[29]

It is possible that the pathways activated, seemingly independently by uPAR and $\alpha v\beta 6$, could indeed be activated collectively with proteins found in membranes forming the uPAR·$\alpha v\beta 6$ complex. Indeed, in our initial study several other proteins were identified by proteomics to be binding to uPAR.[5] Targeting $\alpha v\beta 6$ integrin has the additional benefit that it is exclusively expressed in epithelial restricted tumors. It is possible that by therapeutically targeting the uPAR·$\alpha v\beta 6$, the $\alpha v\beta 6$ signaling pathway can be uncoupled from the plasmin activity, potentially leading to a disruption of the pathways involved in EMT resulting in decreased metastasis.

This study provides the detailed groundwork for an analysis of the uPAR·$\alpha v\beta 6$ interaction aimed at using it as a potential novel therapeutic cancer target. Further alternative and complementary techniques could be used to elucidate P·P interactions and to identify significant pathways affected by the interaction. When combined with the approaches taken here, methods like cross-linking mass spectrometry[54] in conjunction with competition studies using peptide arrays and surface plasmon resonance analysis (e.g., BIAcore, Proteon) could be used to analyze the binding kinetics of potential interactants. Indeed, preliminary studies using complementary peptides to block the sites of binding followed by functional assays (migration, proliferation, etc.) on related cell lines have been shown to induce biological and morphological effects (data not shown). The consequences of ablating such interactions can be investigated in mouse models of CRC enabling an in vivo approach.

AUTHOR INFORMATION

Corresponding Author

*Phone: +61 2 9850 8211. Fax: +61 2 9812-3600. E-mail: mark.baker@mq.edu.au.

Author Contributions

$^{\nabla}$These authors contributed equally.

Notes

The authors declare no competing financial interest.

ACKNOWLEDGMENTS

We thank Paul H. Weinreb and Sheila M. Violette, from Biogen Idec Inc., Cambridge Center, Cambridge, MA 02142, for kindly providing the 6.4B4 antibody against the integrin $\alpha v\beta 6$. This study was supported with research project grant funding from the NHMRC (#1010303), Cancer Council NSW (RG10-04 and RG08-16), and a Macquarie University MQSN grant and supported through the Australian School of Advanced Medicine (ASAM), Macquarie University, MQ Biofocus and Biomolecular Frontiers Research Centres. Some of the research described herein was facilitated by access to the Australian Proteome Analysis Facility (APAF) and Monash University Antibody Technology Facility (MATF), both established under the Australian Government's National Collaborative Research Infrastructure Strategy (NCRIS).

REFERENCES

(1) Nguyen, D. X.; Bos, P. D.; Massague, J. Metastasis: from dissemination to organ-specific colonization. *Nat. Rev. Cancer* **2009**, *9*, 274−84.

(2) Kalluri, R.; Weinberg, R. A. The basics of epithelial-mesenchymal transition. *J. Clin. Invest.* **2009**, *119*, 1420−8.

(3) Pepper, M. S. Role of the matrix metalloproteinase and plasminogen activator-plasmin systems in angiogenesis. *Arterioscler., Thromb., Vasc. Biol.* **2001**, *21*, 1104−17.

(4) Cox, G.; Steward, W. P.; O'Byrne, K. J. The plasmin cascade and matrix metalloproteinases in non-small cell lung cancer. *Thorax* **1999**, *54*, 169−79.

(5) Saldanha, R. G.; Molloy, M. P.; Bdeir, K.; Cines, D. B.; Song, X.; Uitto, P. M.; Weinreb, P. H.; Violette, S. M.; Baker, M. S. Proteomic identification of lynchpin urokinase plasminogen activator receptor protein interactions associated with epithelial cancer malignancy. *J. Proteome Res.* **2007**, *6*, 1016−28.

(6) Fagerberg, L.; Jonasson, K.; von Heijne, G.; Uhlen, M.; Berglund, L. Prediction of the human membrane proteome. *Proteomics* **2010**, *10*, 1141−9.

(7) Smith, H. W.; Marshall, C. J. Regulation of cell signalling by uPAR. *Nat. Rev. Mol. Cell Biol.* **2010**, *11*, 23−36.

(8) Llinas, P.; Le Du, M. H.; Gardsvoll, H.; Dano, K.; Ploug, M.; Gilquin, B.; Stura, E. A.; Menez, A. Crystal structure of the human urokinase plasminogen activator receptor bound to an antagonist peptide. *EMBO J.* **2005**, *24*, 1655−63.

(9) Eden, G.; Archinti, M.; Furlan, F.; Murphy, R.; Degryse, B. The urokinase receptor interactome. *Curr. Pharm. Des.* **2011**, *17*, 1874−89.

(10) Mekkawy, A. H.; Morris, D. L.; Pourgholami, M. H. Urokinase plasminogen activator system as a potential target for cancer therapy. *Future Oncol.* **2009**, *5*, 1487−99.

(11) Seetoo, D. Q.; Crowe, P. J.; Russell, P. J.; Yang, J. L. Quantitative expression of protein markers of plasminogen activation system in prognosis of colorectal cancer. *J. Surg. Oncol.* **2003**, *82*, 184−93.

(12) Rabbani, S. A.; Mazar, A. P. The role of the plasminogen activation system in angiogenesis and metastasis. *Surg. Oncol. Clin. N. Am.* **2001**, *10*, 393−415.

(13) Hynes, R. O. Integrins: versatility, modulation, and signaling in cell adhesion. *Cell* **1992**, *69*, 11−25.

(14) Giancotti, F. G.; Ruoslahti, E. Integrin signaling. *Science* **1999**, *285*, 1028−32.
(15) Liu, S.; Liang, B.; Gao, H.; Zhang, F.; Wang, B.; Dong, X.; Niu, J. Integrin alphavbeta6 as a novel marker for diagnosis and metastatic potential of thyroid carcinoma. *Head Neck Oncol.* **2013**, *5*, 7.
(16) Bandyopadhyay, A.; Raghavan, S. Defining the role of integrin alphavbeta6 in cancer. *Curr. Drug Targets* **2009**, *10*, 645−52.
(17) Bates, R. C. The alphaVbeta6 integrin as a novel molecular target for colorectal cancer. *Future Oncol.* **2005**, *1*, 821−8.
(18) Annes, J. P.; Munger, J. S.; Rifkin, D. B. Making sense of latent TGFbeta activation. *J. Cell Sci.* **2003**, *116*, 217−24.
(19) Gu, X.; Niu, J.; Dorahy, D. J.; Scott, R.; Agrez, M. V. Integrin alpha(v)beta6-associated ERK2 mediates MMP-9 secretion in colon cancer cells. *Br. J. Cancer* **2002**, *87*, 348−51.
(20) Weinreb, P. H.; Simon, K. J.; Rayhorn, P.; Yang, W. J.; Leone, D. R.; Dolinski, B. M.; Pearse, B. R.; Yokota, Y.; Kawakatsu, H.; Atakilit, A.; Sheppard, D.; Violette, S. M. Function-blocking integrin alpha(v)-beta(6) monoclonal antibodies - Distinct ligand-mimetic and non-ligand-mimetic classes. *J. Biol. Chem.* **2004**, *279*, 17875−17887.
(21) Tsao, S. W.; Mok, S. C.; Fey, E. G.; Fletcher, J. A.; Wan, T. S.; Chew, E. C.; Muto, M. G.; Knapp, R. C.; Berkowitz, R. S. Characterization of human ovarian surface epithelial cells immortalized by human papilloma viral oncogenes (HPV-E6E7 ORFs). *Exp. Cell Res.* **1995**, *218*, 499−507.
(22) Agrez, M.; Chen, A.; Cone, R. I.; Pytela, R.; Sheppard, D. The alpha v beta 6 integrin promotes proliferation of colon carcinoma cells through a unique region of the beta 6 cytoplasmic domain. *J. Cell Biol.* **1994**, *127*, 547−56.
(23) Weinacker, A.; Chen, A.; Agrez, M.; Cone, R. I.; Nishimura, S.; Wayner, E.; Pytela, R.; Sheppard, D. Role of the integrin alpha v beta 6 in cell attachment to fibronectin. Heterologous expression of intact and secreted forms of the receptor. *J. Biol. Chem.* **1994**, *269*, 6940−8.
(24) Frank, R. The SPOT-synthesis technique. Synthetic peptide arrays on membrane supports–principles and applications. *J. Immunol. methods* **2002**, *267*, 13−26.
(25) Frank, R. Spot-Synthesis - an easy technique for the positionally addressable, parallel chemical synthesis on a membrane support. *Tetrahedron* **1992**, *48*, 9217−9232.
(26) Huai, Q.; Zhou, A.; Lin, L.; Mazar, A. P.; Parry, G. C.; Callahan, J.; Shaw, D. E.; Furie, B.; Furie, B. C.; Huang, M. Crystal structures of two human vitronectin, urokinase and urokinase receptor complexes. *Nat. Struct. Mol. Biol.* **2008**, *15*, 422−3.
(27) Abagyan, R.; Totrov, M.; Kuznetsov, D. ICM−A new method for protein modeling and design: Applications to docking and structure prediction from the distorted native conformation. *J. Comput. Chem.* **1994**, *15*, 488−506.
(28) Li, Y.; Wood, N.; Yellowlees, D.; Donnelly, P. K. Cell surface expression of urokinase receptor in normal mammary epithelial cells and breast cancer cell lines. *Anticancer Res.* **1999**, *19*, 1223−8.
(29) Ahmed, N.; Niu, J.; Dorahy, D. J.; Gu, X.; Andrews, S.; Meldrum, C. J.; Scott, R. J.; Baker, M. S.; Macreadie, I. G.; Agrez, M. V. Direct integrin alphavbeta6-ERK binding: implications for tumour growth. *Oncogene* **2002**, *21*, 1370−80.
(30) Niu, J.; Gu, X.; Ahmed, N.; Andrews, S.; Turton, J.; Bates, R.; Agrez, M. The alphaVbeta6 integrin regulates its own expression with cell crowding: implications for tumour progression. *Int. J. Cancer* **2001**, *92*, 40−8.
(31) Moreau, M.; Mourah, S.; Dosquet, C. beta-Catenin and NF-kappaB cooperate to regulate the uPA/uPAR system in cancer cells. *Int. J. Cancer* **2011**, *128*, 1280−92.
(32) Ronne, E.; Behrendt, N.; Ploug, M.; Nielsen, H. J.; Wollisch, E.; Weidle, U.; Dano, K.; Hoyer-Hansen, G. Quantitation of the receptor for urokinase plasminogen activator by enzyme-linked immunosorbent assay. *J. Immunol. Methods* **1994**, *167*, 91−101.
(33) Persson, M.; Madsen, J.; Ostergaard, S.; Jensen, M. M.; Jorgensen, J. T.; Juhl, K.; Lehmann, C.; Ploug, M.; Kjaer, A. Quantitative PET of human urokinase-type plasminogen activator receptor with 64Cu-DOTA-AE105: implications for visualizing cancer invasion. *J. Nucl. Med.* **2012**, *53*, 138−45.
(34) Weibrecht, I.; Leuchowius, K. J.; Clausson, C. M.; Conze, T.; Jarvius, M.; Howell, W. M.; Kamali-Moghaddam, M.; Soderberg, O. Proximity ligation assays: a recent addition to the proteomics toolbox. *Expert Rev. Proteomics* **2010**, *7*, 401−9.
(35) Thymiakou, E.; Episkopou, V. Detection of signaling effector-complexes downstream of bmp4 using PLA, a proximity ligation assay. *J. Visualized Exp.* **2011**.
(36) Breuss, J. M.; Gillett, N.; Lu, L.; Sheppard, D.; Pytela, R. Restricted distribution of integrin beta 6 mRNA in primate epithelial tissues. *J. Histochem. Cytochem.* **1993**, *41*, 1521−7.
(37) Li, S. S.; Wu, C. Using peptide array to identify binding motifs and interaction networks for modular domains. *Methods Mol. Biol.* **2009**, *570*, 67−76.
(38) Maier, R. H.; Maier, C. J.; Rid, R.; Hintner, H.; Bauer, J. W.; Onder, K. Epitope mapping of antibodies using a cell array-based polypeptide library. *J. Biomol. Screening* **2010**, *15*, 418−26.
(39) Barinka, C.; Parry, G.; Callahan, J.; Shaw, D. E.; Kuo, A.; Bdeir, K.; Cines, D. B.; Mazar, A.; Lubkowski, J. Structural basis of interaction between urokinase-type plasminogen activator and its receptor. *J. Mol. Biol.* **2006**, *363*, 482−95.
(40) Chaurasia, P.; Aguirre-Ghiso, J. A.; Liang, O. D.; Gardsvoll, H.; Ploug, M.; Ossowski, L. A region in urokinase plasminogen receptor domain III controlling a functional association with alpha5beta1 integrin and tumor growth. *J. Biol. Chem.* **2006**, *281*, 14852−63.
(41) Vassalli, J. D.; Baccino, D.; Belin, D. A cellular binding site for the Mr 55,000 form of the human plasminogen activator, urokinase. *J. Cell Biol.* **1985**, *100*, 86−92.
(42) Blasi, F.; Carmeliet, P. uPAR: a versatile signalling orchestrator. *Nat. Rev. Mol. Cell Biol.* **2002**, *3*, 932−43.
(43) Sowmya, G.; Khan, J. M.; Anand, S.; Ahn, S. B.; Baker, M. S.; Ranganathan, S. A site for direct integrin alphavbeta6.uPAR interaction from structural modelling and docking. *J. Struct. Biol.* **2014**, *185*, 327−35.
(44) Hruby, V. J. Designing peptide receptor agonists and antagonists. *Nat. Rev. Drug Discovery* **2002**, *1*, 847−58.
(45) Jo, M.; Eastman, B. M.; Webb, D. L.; Stoletov, K.; Klemke, R.; Gonias, S. L. Cell signaling by urokinase-type plasminogen activator receptor induces stem cell-like properties in breast cancer cells. *Cancer Res.* **2010**, *70*, 8948−58.
(46) Smith, H. W.; Marra, P.; Marshall, C. J. uPAR promotes formation of the p130Cas-Crk complex to activate Rac through DOCK180. *J. Cell Biol.* **2008**, *182*, 777−90.
(47) Degryse, B.; Orlando, S.; Resnati, M.; Rabbani, S. A.; Blasi, F. Urokinase/urokinase receptor and vitronectin/alpha(v)beta(3) integrin induce chemotaxis and cytoskeleton reorganization through different signaling pathways. *Oncogene* **2001**, *20*, 2032−43.
(48) Bates, R. C. Colorectal cancer progression: integrin alphavbeta6 and the epithelial-mesenchymal transition (EMT). *Cell Cycle* **2005**, *4*, 1350−2.
(49) Ramos, D. M.; But, M.; Regezi, J.; Schmidt, B. L.; Atakilit, A.; Dang, D.; Ellis, D.; Jordan, R.; Li, X. Expression of integrin beta 6 enhances invasive behavior in oral squamous cell carcinoma. *Matrix Biol.* **2002**, *21*, 297−307.
(50) Li, X.; Yang, Y.; Hu, Y.; Dang, D.; Regezi, J.; Schmidt, B. L.; Atakilit, A.; Chen, B.; Ellis, D.; Ramos, D. M. Alphavbeta6-Fyn signaling promotes oral cancer progression. *J. Biol. Chem.* **2003**, *278*, 41646−53.
(51) Ramos, D. M.; Dang, D.; Sadler, S. The role of the integrin alpha v beta6 in regulating the epithelial to mesenchymal transition in oral cancer. *Anticancer Res.* **2009**, *29*, 125−30.
(52) Morgan, M. R.; Thomas, G. J.; Russell, A.; Hart, I. R.; Marshall, J. F. The integrin cytoplasmic-tail motif EKQKVDLSTDC is sufficient to promote tumor cell invasion mediated by matrix metalloproteinase (MMP)-2 or MMP-9. *J. Biol. Chem.* **2004**, *279*, 26533−9.
(53) Xu, J.; Lamouille, S.; Derynck, R. TGF-beta-induced epithelial to mesenchymal transition. *Cell Res.* **2009**, *19*, 156−72.
(54) Tang, X.; Bruce, J. E. A new cross-linking strategy: protein interaction reporter (PIR) technology for protein-protein interaction studies. *Mol. BioSyst.* **2010**, *6*, 939−47.